Research Article

Journal of Molecular Recognition

Received: 6 July 2010, Revised: 26 July 2010, Accepted: 26 July 2010, Published online in Wiley Online Library: 14 December 2010

(wileyonlinelibrary.com) DOI:10.1002/jmr.1080

Binding of the cSH3 domain of Grb2 adaptor to two distinct RXXK motifs within Gab1 docker employs differential mechanisms

Caleb B. McDonald[a], Kenneth L. Seldeen[a], Brian J. Deegan[a], Vikas Bhat[a] and Amjad Farooq[a]*

A ubiquitous component of cellular signaling machinery, Gab1 docker plays a pivotal role in routing extracellular information in the form of growth factors and cytokines to downstream targets such as transcription factors within the nucleus. Here, using isothermal titration calorimetry (ITC) in combination with macromolecular modeling (MM), we show that although Gab1 contains four distinct RXXK motifs, designated G1, G2, G3, and G4, only G1 and G2 motifs bind to the cSH3 domain of Grb2 adaptor and do so with distinct mechanisms. Thus, while the G1 motif strictly requires the PPRPPKP consensus sequence for high-affinity binding to the cSH3 domain, the G2 motif displays preference for the PXVXRXLKPXR consensus. Such sequential differences in the binding of G1 and G2 motifs arise from their ability to adopt distinct polyproline type II (PPII)- and 3_{10}-helical conformations upon binding to the cSH3 domain, respectively. Collectively, our study provides detailed biophysical insights into a key protein–protein interaction involved in a diverse array of signaling cascades central to health and disease. Copyright © 2010 John Wiley & Sons, Ltd.

Keywords: Grb2 adaptor; Gab1 docker; SH3-ligand thermodynamics; isothermal titration calorimetry; macromolecular modeling

INTRODUCTION

Gab1 is a cellular protein that mediates signaling between cell surface receptor tyrosine kinases (RTKs) and downstream molecules such as Ras and Akt by virtue of its ability to act as a docking platform for a multitude of adaptors and enzymes (Liu and Rohrschneider, 2002; Gu and Neel, 2003; Nishida and Hirano, 2003). The modular design of Gab1, comprised an N-terminal pleckstrin homology (PH) domain and a C-terminal proline-rich (PR) domain, underscores its central role in a diverse array of signaling cascades central to health and disease. The disruption of gab1 gene results in numerous developmental defects in mice and its over-expression is implicated in the genesis of human breast cancer (Itoh *et al*., 2000; Sachs *et al*., 2000; Daly *et al*., 2002; Brummer *et al*., 2006; Ke *et al*., 2007; Bennett *et al*., 2008). The ability of Gab1 to orchestrate such key cellular functions is heavily dependent upon its recruitment to the inner membrane surface by its upstream partner Grb2.

Comprised of a central SH2 domain flanked between N-terminal SH3 (nSH3) and C-terminal SH3 (cSH3) domains (Figure 1a), Grb2 recognizes activated cell surface RTKs such as HGFR, EGFR, FGFR, and PDGFR by virtue of its SH2 domain's ability to bind to tyrosine-phosphorylated (pY) sequences in the context of pYXN motifs located within the receptor tails on the cytoplasmic face of the membrane (Lowenstein *et al*., 1992; Rozakis-Adcock *et al*., 1992). Upon binding to RTKs, the SH3 domains of Grb2 recruit a wide variety of proteins containing proline-rich sequences to the inner membrane surface – the site of initiation of a multitude of signaling cascades (Chardin *et al*., 1993; Li *et al*., 1993; Seedorf *et al*., 1994; Odai *et al*., 1995; Park *et al*., 1998; Vidal *et al*., 1998; Schaeper *et al*., 2000; Lewitzky *et al*., 2001; Moeller *et al*., 2003). Among them, the Sos1 guanine nucleotide exchange factor and the Gab1 docker are by far the best characterized downstream partners of Grb2 (Chardin *et al*., 1993; Li *et al*., 1993; Schaeper *et al*., 2000; Lewitzky *et al*., 2001). Upon recruitment to the inner membrane surface, Sos1 facilitates the GDP–GTP exchange within the membrane-bound Ras GTPase and thereby switches on a key signaling circuit that involves the activation of MAPK cascade central to cellular growth and proliferation (Robinson and Cobb, 1997). In contrast, the recruitment of Gab1 to the inner membrane surface provides docking platforms for the Shp2 tyrosine phosphatase and the PI3K lipid kinase, which, respectively, account for further amplification of Ras activity, as sustained activation of Ras requires both the Sos1-dependent and Gab1-dependent pathways (Cunnick *et al*., 2002; Araki *et al*., 2003; Gu and Neel, 2003), and the activation of Akt serine–threonine kinase, which plays an important role in cell growth and survival (Kim and Chung, 2002).

* *Correspondence to: A. Farooq, Department of Biochemistry & Molecular Biology, USylvester Braman Family Breast Cancer Institute, Leonard Miller School of Medicine, University of Miami, Miami, FL 33136, USA.*
E-mail: amjad@farooqlab.net

a *C. B. McDonald, K. L. Seldeen, B. J. Deegan, V. Bhat, A. Farooq*
Department of Biochemistry & Molecular Biology, USylvester Braman Family Breast Cancer Institute, Leonard Miller School of Medicine, University of Miami, Miami, FL 33136, USA

Abbreviations used: *CD, circular dichroism; EGFR, epidermal growth factor receptor; FGFR, fibroblast growth factor receptor; Gab1, Grb2-associated binder 1; Grb2, growth factor receptor binder 2; HGFR, hepatocyte growth factor receptor; ITC, isothermal titration calorimetry; MAPK, mitogen-activated protein kinase; MM, macromolecular modeling; PDGFR, platelet-derived growth factor receptor; PPII, polyproline type II; RTK, receptor tyrosine kinase; SEC, size-exclusion chromatography; SH2, Src homology 2; SH3Src homology 3; Sos1, son of sevenless 1.*

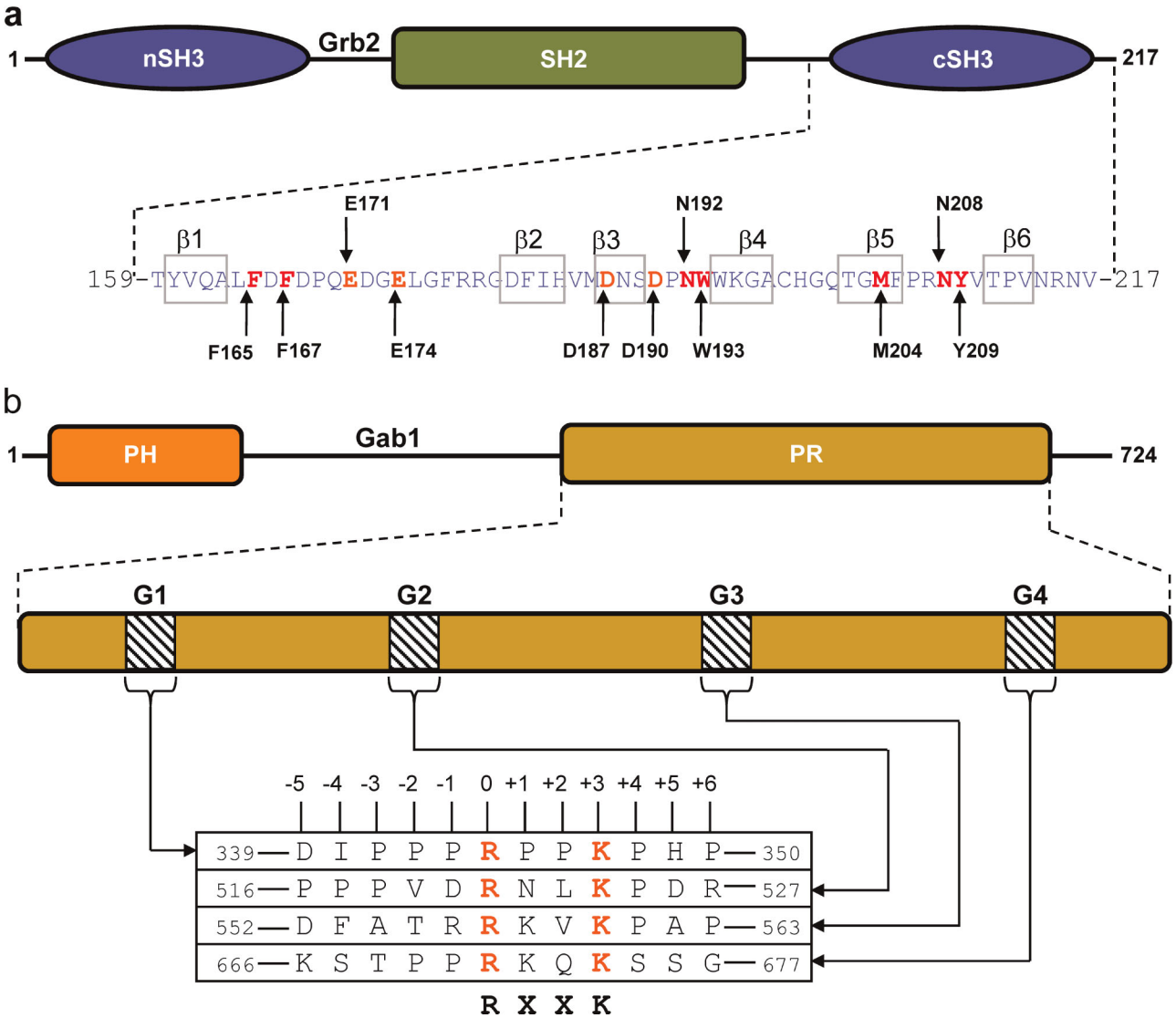

Figure 1. Modular organization of Grb2 adaptor and Gab1 docker. (a) Grb2 is composed of a central SH2 (Src homology 2) domain flanked between an N-terminal SH3 (nSH3) domain and a C-terminal SH3 (cSH3) domain. The amino acid sequence of the cSH3 domain is indicated with the residues constituting the β1–β6 strands clearly demarcated. Key amino acid residues within the cSH3 domain involved in recognition of cognate ligands are colored red and labeled for clarity. (b) Gab1 is constructed on an N-terminal PH (Pleckstrin homology) domain and a C-terminal proline-rich (PR) domain separated by a long stretch of uncharacterized region. The PR domain contains four distinct RXXK motifs, here designated as G1, G2, G3, and G4. The amino acid sequence of these motifs and flanking residues within Gab1 is provided. The numbering of various residues within and flanking the RXXK motifs is based on the nomenclature suggested by Feller and co-workers (Harkiolaki *et al.*, 2009).

The Grb2–Gab1 interaction is believed to occur through the binding of cSH3 domain of Grb2 to an atypical RXXK motif within the PR domain of Gab1 (Lock *et al.*, 2000; Lewitzky *et al.*, 2001). However, the PR domain of Gab1 contains four such motifs, herein designated G1, G2, G3, and G4 (Figure 1b), raising the possibility that there may be multiple docking sites within Gab1 for accommodating Grb2. Such a scenario could translate into the assembly of higher order Grb2–Gab1 multimers rather than a simple binary complex. In an attempt to further our understanding of the assembly of Grb2–Gab1 signaling complex, the present study was undertaken. Using isothermal titration calorimetry (ITC) in combination with macromolecular modeling (MM), we show that only G1 and G2 motifs within Gab1 bind to the cSH3 domain of Grb2 adaptor and do so with distinct mechanisms. Thus, while the G1 motif strictly requires the PPRPPKP consensus sequence for high-affinity binding to the cSH3 domain, the G2 motif displays preference for the PXVXRXLKPXR consensus. Such sequential differences in the binding of G1 and G2 motifs arise from their ability to adopt distinct polyproline type II (PPII)- and 3_{10}-helical conformations upon binding to the cSH3 domain, respectively. Collectively, our study provides detailed biophysical insights into a key protein–protein interaction involved in a diverse array of signaling cascades central to health and disease.

MATERIALS AND METHODS

Sample preparation

pET102 bacterial expression plasmids for wild-type and mutant cSH3 domains of human Grb2 were cloned and expressed in *Escherichia coli* Rosetta2(DE3) strain as described earlier (McDo-

nald *et al*., 2008a, 2009). Recombinant proteins were purified to apparent homogeneity using a combination of Ni-NTA and size-exclusion chromatographic procedures and further characterized as reported previously (McDonald *et al*., 2008a, 2009). 12-mer wild-type and mutant peptides spanning G1, G2, G3, and G4 sites within human Gab1 were commercially obtained from GenScript Corporation. The sequences of these peptides are shown in Figure 1b. The peptide concentrations were measured gravimetrically. Circular dichroism (CD) analysis of cSH3 domains and Gab1 peptides revealed that the introduction of various alanine substitutions at specific positions had no major effect on their secondary structural conformations.

ITC measurements

ITC experiments were performed on a Microcal VP-ITC instrument and data were acquired and processed using fully automized features in Microcal ORIGIN software. All measurements were repeated 3–4 times. Briefly, SH3 domain samples were prepared in 50 mM Tris, 1 mM EDTA, and 5 mM β-mercaptoethanol at pH 8.0 containing 0–500 mM NaCl. The experiments were initiated by injecting 25× 10 μl aliquots of 2–8 mM of each peptide from the syringe into the calorimetric cell containing 1.8 ml of 50–200 μM of an cSH3 domain solution at 25°C. All other control experiments were performed as described earlier (McDonald *et al*., 2008a, 2009). To extract binding affinity (K_d) and binding enthalpy (ΔH), the ITC isotherms were iteratively fit to the following built-in function by nonlinear least-squares regression analysis using the integrated ORIGIN software:

$$q(i) = \left(\frac{n\Delta HVP}{2}\right) \left\{\left[1 + \left(\frac{L}{nP}\right) + \left(\frac{K_d}{nP}\right)\right] - \left[\left[1 + \left(\frac{L}{nP}\right) + \left(\frac{K_d}{nP}\right)\right]^2 - \left(\frac{4L}{nP}\right)\right]^{1/2}\right\} \quad (1)$$

where $q(i)$ is the heat release (kcal/mol) for the ith injection, n is the binding stoichiometry, V is the effective volume of protein solution in the calorimetric cell (1.46 ml), P is the total protein concentration in the calorimetric cell, and L is the total concentration of peptide ligand added for the ith injection. The above equation is derived from the binding of a ligand to a macromolecule using the law of mass action assuming a one-site model (Wiseman *et al*., 1989). The free energy change (ΔG) upon ligand binding was calculated from the relationship:

$$\Delta G = RT \ln K_d \quad (2)$$

where R is the universal molar gas constant (1.99 cal/K/mol) and T is the absolute temperature. The entropic contribution ($T\Delta S$) to the free energy of binding was calculated from the relationship:

$$T\Delta S = \Delta H - \Delta G \quad (3)$$

where ΔH and ΔG are as defined above. The free energy change (ΔG) upon ligand binding can be dissected into two major constituent components by the following relationship:

$$\Delta G = \Delta G_{lig} + \Delta G_{ion} \quad (4)$$

where ΔG_{lig} is the contribution due to direct ligand binding and ΔG_{ion} is the contribution due to the indirect displacement of counterions upon ligand binding. ΔG_{ion} at a given NaCl concentration was calculated from the following relationship based on the polyelectrolyte theory (Wyman, 1964; Record *et al*., 1976; Lohman and Mascotti, 1992; Chaires, 1996):

$$\Delta G_{ion} = \psi RT \ln[\mathrm{NaCl}] \quad (5)$$

where ψ is the fractional degree of net counterions displaced upon ligand binding. ψ was calculated from the slope of a plot of $\ln K_d$ versus ln[NaCl] assuming the following linear relationship based on thermodynamic linkage (Wyman, 1964; Record *et al*., 1976; Lohman and Mascotti, 1992; Chaires, 1996):

$$\ln K_d = \psi \ln[\mathrm{NaCl}] + \ln K_0 \quad (6)$$

where ψ and $\ln K_0$ are the slope and the y-intercept of $\ln K_d - \ln[\mathrm{NaCl}]$ plot, respectively. With the knowledge of ΔG and ΔG_{ion}, Equation (4) was re-arranged to obtain ΔG_{lig}. It is noteworthy that in order to ascertain greater confidence in the accuracy of thermodynamic parameters determined using ITC, it is desirable for measurements to be conducted under conditions where the experimental window of $5 < c < 500$ is met. The c-value is a dimensionless parameter defined as the ratio of protein concentration (μM) in the calorimetric cell to the equilibrium dissociation constant (μM) for the binding of an appropriate ligand or peptide. Simply put, the c-value constraint simply arises from the basic fact that the protein concentration in the calorimetric cell should be ideally between 5-fold to 500-fold higher than the equilibrium dissociation constant. However, for low-affinity systems, as the one under study here, it is not always possible to work in the experimental window of $5 < c < 500$ due to the requirement of rather large concentrations of both the protein and the ligand. Indeed, concentrations of various constructs of the cSH3 domain and peptides employed in this study were just below the levels at which they were either prone to aggregation or subject to insolubility. In light of such experimental limitations, the experimental window of $5 < c < 500$ was not met in this study. Nonetheless, a rather high accuracy of thermodynamic parameters reported here can be expected due to the fulfillment of following conditions: (1) the ITC isotherms were obtained over a large titration window and allowed to reach near-saturation; (2) the concentrations of both the protein and the peptides were determined with high accuracy; (3) the signal-to-noise ratio was excellent and typically close to 100; and (4) the stoichiometry of binding was known to be 1:1 for all experiments. Provided that the above conditions are met, a recent study indeed indicates that accurate thermodynamic parameters can be obtained for low-affinity systems even when working outside the experimental window of $5 < c < 500$ (Turnbull and Daranas, 2003).

Macromolecular modeling

MM was employed to obtain 3D structures of the cSH3 domain of Grb2 in complex with peptides containing the G1 and G2 motifs located within the PR domain of Gab1 using the MODELLER software based on homology modeling (Marti-Renom *et al*., 2000). For the structure of cSH3 domain in complex with G1 peptide, the crystal structure of cSH3 domain of Grb2 bound to a peptide derived from a homologous site in Gab2 containing the PPRPPKP motif was used as a template (PDB# 2W0Z). For the structure of cSH3 domain in complex with G2 peptide, the crystal structure of cSH3 domain of Grb2 bound to a peptide derived from a homologous site in Gab2 containing the PXVXRXLKPXR motif was used as a template (PDB# 2VWF). Briefly, MODELLER employs molecular dynamics and simulated annealing protocols to optimize the modeled structure through satisfaction of spatial

restraints derived from amino acid sequence alignment with a corresponding template in Cartesian space. For amino acid sequence identity between 25% and 50% between the template and target, MODELLER can generate 3D structures with accuracy comparable to NMR and X-ray structures for small proteins such as SH3 domains of around 50 amino acid (John and Sali, 2003). Importantly, the PPRPPKP and PXVXRXLKPXR motifs in Gab1 share over 90% sequence identity with the corresponding motifs in Gab2, while the cSH3 domain is identical between the template and target structures. Thus, the modeled structures of cSH3 domain of Grb2 in complex with G1 and G2 peptides derived from Gab1 would be expected to adopt 3D folds fairly similar to the template structures except for the side chain conformations of specific amino acids. This is due to the introduction of specific hydrogen bonding restraints between specific pairs of basic residues in the G1 peptide or the G2 peptide and acidic residues in the cSH3 domain. Introduction of such hydrogen bonding restraints was necessary to bring the side chain atoms of respective residues within optimal hydrogen bonding distance in agreement with our thermodynamic data reported here. The atomic distances set for hydrogen bonding restraints between a specific pair of oxygen and nitrogen atoms were 2.8 ± 0.5 Å. Thus, MODELLER will force the side chain oxygen and nitrogen atoms of specific hydrogen bonding partners to lie within approximately 2.8 Å of each other through the rotation of backbone N–Cα and Cα–C$'$ bonds with little effect on the overall 3D fold of cSH3 domain in complex with G1 peptide or G2 peptide. To generate the 3D structural models of cSH3 domain in complex with the G1 and G2 peptides, hydrogen bonding restraints were, respectively, added between OE1 and OE2 atoms of E171 and NH1/NH2 atoms of R0, between OE1 and OE2 atoms of E171 and NH1/NH2 atoms of K + 3, between OE1 and OE2 atoms of E174 and NH1/NH2 atoms of R0, and between OE1 and OE2 atoms of E174 and NH1 and NH2 atoms of K + 3. Additionally, hydrogen bonding restraints were also added between OD1/OD2 atoms of D187 and NH1/NH2 atoms of R + 6, and between OD1/OD2 atoms of D190 and NH1/NH2 atoms of R + 6 for the 3D structural model of cSH3 domain in complex with G2 peptide. In each case, a total of 100 structural models were calculated and the structure with the lowest energy, as judged by the MODELLER Objective Function, was selected for further analysis. The modeled structures were rendered using RIBBONS (Carson, 1991).

RESULTS AND DISCUSSION

cSH3 domain binds exclusively to G1 and G2 motifs within Gab1

In an attempt to elucidate how Grb2 and Gab1 interact, we tested the binding of cSH3 domain of Grb2 to four putative sites G1–G4, containing RXXK motifs, within the PR domain of Gab1 using ITC. Figure 2 shows representative data obtained from such measurements. The complete thermodynamic profiles are provided in Table 1. It is immediately apparent that while the cSH3 domain binds to G1 and G2 sites with affinities in the physiologically relevant tens to hundreds of micromolar range, no binding is observed to G3 and G4 sites under identical conditions. Varying the conditions of ITC experiments such as temperature, pH, or ionic strength had no effect on these observations, implying that the G3 and G4 motifs indeed lack intrinsic affinity for the cSH3 domain in lieu of lack of any observable change in the heat of binding. We note that the rather weak affinities observed here are ideally suited for players involved in orchestrating the highly transient and reversible nature of signaling cascades and are in line with the weak binding nature of other SH3–ligand interactions (Feng *et al*., 1994; Lim *et al*., 1994; Yu *et al*., 1994; Sparks *et al*., 1996; Brannetti *et al*., 2000; Ghose *et al*., 2001; Mayer, 2001; Cesareni *et al*., 2002; Panni *et al*., 2002; Tong *et al*., 2002; Zarrinpar *et al*., 2003). Interestingly, the G2 motif binds to the cSH3 domain with an affinity that is over threefold stronger than that observed for the G1 motif, suggesting that Gab1 contains a high-affinity and a low-affinity site for Grb2. It is also noteworthy that the binding of G1 and G2 motifs to the cSH3 domain employs distinct thermodynamic mechanisms (Table 1). Thus, while the binding of G1 motif is driven by both favorable enthalpic and entropic contributions to the overall free energy, the binding of G2 motif is exclusively driven by favorable enthalpic forces accompanied by an entropic penalty. Importantly, the fact that the cSH3 domain does not bind to G3 and G4 sites suggests that residues within or flanking the RXXK motifs are likely to add an additional element of specificity between Grb2 and Gab1. In light of the observation that alanine substitution of P − 4 residue within the G2 site of Gab1 abrogates its binding to the cSH3 domain of Grb2 (Lock *et al*., 2000; Lewitzky *et al*., 2001), we reasoned that the lack of a proline at the −4 position could account for the lack of binding of the cSH3 domain to G3 and G4 sites. However, an isoleucine at the −4 position within the G1 site could partially substitute for the role of a proline at this position within the G2 site due to the hydrophobicity and non-bulky character of its side chain moiety, while phenyl alanine and serine at the −4 position within the G3 and G4 sites may not be able to do so. To test our hypothesis, we introduced isoleucine (G2_P − 4I), phenyl alanine (G2_P − 4F), and serine (G2_P − 4S) at the −4 position within the G2 peptide and measured the binding of resulting mutant peptides to the cSH3 domain (Table 1). Interestingly, while the G2_P − 4F and G2_P − 4S peptides showed no binding to the cSH3 domain, the G2_P − 4I peptide bound with an affinity over an order of magnitude lower than that observed for the binding of G2 peptide. Collectively, these observations imply that the presence of an isoleucine at the −4 position cannot account for the binding of cSH3 domain to G1 site relative to G3 and G4 sites and that the binding of cSH3 domain to G1 and G2 sites may be governed by distinct molecular determinants.

G1 and G2 motifs employ distinct consensus sequences to recognize the cSH3 domain

The data presented above suggest that specific residues within and flanking the RXXK motifs must also dictate the binding of G1 and G2 sites to the cSH3 domain. In an effort to understand the molecular determinants of the binding of cSH3 domain to G1 and G2 sites but not to G3 and G4, we conducted full-scale alanine scan of both the G1 and G2 peptides (Tables 2 and 3). Our data reveal that alanine substitution of residues at positions −2, 0, +1, and +3 within the G1 peptide either completely abolishes binding or results in the reduction of binding affinity that cannot be accurately quantified, implying that these residues are critical. Additionally, alanine substitution of residues at positions −1, +2, and +4 within the G1 peptide compromises binding affinity by over threefold, implying that these residues are also obligatory for high-affinity binding of G1 peptide to the cSH3 domain. In

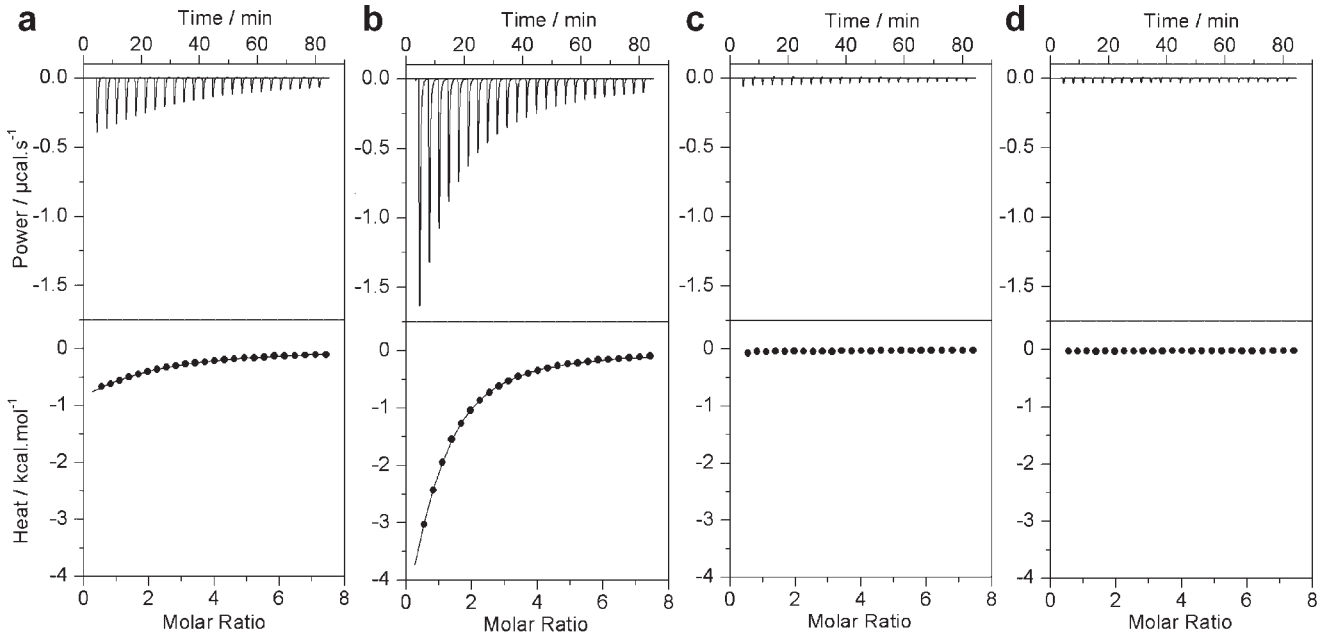

Figure 2. Representative ITC isotherms for the binding of cSH3 domain of Grb2 to Gab1-derived peptides G1 (a), G2 (b), G3 (c), and G4 (d). The upper panels show the raw ITC data expressed as change in thermal power with respect to time over the period of titration. In the lower panels, change in molar heat is expressed as a function of molar ratio of corresponding Gab1 peptide to cSH3 domain of Grb2. The solid lines in the lower panels show the fit of data to a one-site model, as embodied in Equation (1), using the ORIGIN software. Note that all data are shown to same scale for direct comparison.

striking contrast, the critical residues within G2 peptide reside at positions −4, −2, 0, +3, and +4 as their alanine substitutions reduce the binding affinity by either over an order of magnitude or completely abolish binding, while residues at positions +2 and +6 also appear to be important as their substitutions to alanine lead to at least threefold drop in binding affinity. On the basis of these observations, we conclude that the cSH3 domain, respectively, requires PPRPPKP and PXVXRXLKPXR motifs within the G1 and G2 sites in Gab1 for optimal binding. It is thus evident that the binding of cSH3 domain to G1 and G2 sites employs distinct mechanisms. Notably, while residues at positions −2 consecutively through to +4 are required for optimal binding at G1 site, residues at positions −1 and +1 are not required for binding at G2 site but rather residues at positions −4 and +6 fulfill such role.

Acidic residues within the cSH3 domain contribute differentially to the binding of G1 and G2 peptides

Our previous work on the analysis of the binding of cSH3 domain of Grb2 to its putative site within Sos1 has shown that the three acidic residues – E171, D187, and D190 – lining the binding groove within the cSH3 domain engage in the formation of intermolecular salt bridges and are critically required for the recognition of Sos1 (McDonald *et al*., 2008a, 2009). Additionally, structural studies on cSH3 domain of Grb2 and peptides

Table 1. Thermodynamic parameters for the binding of cSH3 domain of Grb2 to wild-type and various mutant Gab1-derived peptides

Peptide	Sequence	*n*	K_d (μM)	ΔH (kcal/mol)	$T\Delta S$ (kcal/mol)	ΔG (kcal/mol)
G1	DIPPP**R**PP**K**PHP	1.05 ± 0.02	152 ± 6	−3.22 ± 0.12	+1.99 ± 0.09	−5.21 ± 0.02
G2	PPPVD**R**NL**K**PDR	0.94 ± 0.01	42 ± 1	−9.63 ± 0.05	−3.65 ± 0.03	−5.97 ± 0.02
G3	DFATR**R**KV**K**PAP	NBD	NBD	NBD	NBD	NBD
G4	KSTPP**R**KQ**K**SSG	NBD	NBD	NBD	NBD	NBD
G2_P − 4I	PIPVD**R**NL**K**PDR	0.92 ± 0.09	564 ± 69	−6.22 ± 0.31	−1.78 ± 0.38	−4.44 ± 0.07
G2_P − 4F	PFPVD**R**NL**K**PDR	NBD	NBD	NBD	NBD	NBD
G2_P − 4S	PSPVD**R**NL**K**PDR	NBD	NBD	NBD	NBD	NBD

The conserved residues within the RXXK motif in each peptide are bold-faced. All parameters were obtained from ITC measurements in a buffer of 50 mM Tris, 200 mM NaCl, 1 mM EDTA, and 5 mM β-mercaptoethanol at pH 8.0 and 25°C. The mutated residues within the G2 peptide are underlined for clarity. NBD indicates no binding determined for the particular peptides either due to lack of any observable heat change or due to poor accuracy of ITC analysis involving such weak interactions ($K_d > 1$ mM). Errors were calculated from 3–4 independent measurements conducted at varying concentrations of cSH3 domain (50–200 μM) and peptides (2–8 mM) in order to further improve the accuracy of thermodynamic parameters. All errors are given to 1 standard deviation.

Table 2. Thermodynamic parameters for the binding of cSH3 domain of Grb2 to single alanine mutants of Gab1-derived G1 peptide

Peptide	Sequence	*n*	K_d (μM)	ΔH (kcal/mol)	$T\Delta S$ (kcal/mol)	ΔG (kcal/mol)
G1	DIP**P**P**R**PP**K**PHP	1.05 ± 0.02	152 ± 6	−3.22 ± 0.12	+1.99 ± 0.09	−5.21 ± 0.02
G1_D − 5A	AIP**P**P**R**PP**K**PHP	1.02 ± 0.04	179 ± 10	−4.63 ± 0.16	+0.49 ± 0.16	−5.12 ± 0.01
G1_I − 4A	DAP**P**P**R**PP**K**PHP	0.97 ± 0.14	323 ± 29	−10.54 ± 0.54	−5.77 ± 0.49	−4.77 ± 0.05
G1_P − 3A	DIA**P**P**R**PP**K**PHP	0.99 ± 0.23	365 ± 47	−10.57 ± 1.45	−5.87 ± 1.37	−4.70 ± 0.08
G1_P − 2A	DIP**A**P**R**PP**K**PHP	NBD	NBD	NBD	NBD	NBD
G1_P − 1A	DIP**P**A**R**PP**K**PHP	1.02 ± 0.03	591 ± 46	−14.47 ± 0.45	−10.06 ± 0.50	−4.41 ± 0.05
G1_R0A	DIP**P**P**A**PP**K**PHP	NBD	NBD	NBD	NBD	NBD
G1_P + 1A	DIP**P**P**R**AP**K**PHP	NBD	NBD	NBD	NBD	NBD
G1_P + 2A	DIP**P**P**R**PA**K**PHP	1.09 ± 0.08	968 ± 71	−18.80 ± 0.41	−14.68 ± 0.45	−4.12 ± 0.04
G1_K + 3A	DIP**P**P**R**PP**A**PHP	NBD	NBD	NBD	NBD	NBD
G1_P + 4A	DIP**P**P**R**PP**K**AHP	1.08 ± 0.02	486 ± 38	−10.52 ± 0.29	−5.99 ± 0.34	−4.53 ± 0.05
G1_H + 5A	DIP**P**P**R**PP**K**PAP	1.00 ± 0.01	157 ± 6	−6.18 ± 0.18	−0.98 ± 0.20	−5.19 ± 0.02
G1_P + 6A	DIP**P**P**R**PP**K**PHA	1.01 ± 0.01	295 ± 7	−10.51 ± 0.23	−5.69 ± 0.24	−4.82 ± 0.01

The conserved residues within the PXRXXK motif in each peptide are bold-faced. All parameters were obtained from ITC measurements in a buffer of 50 mM Tris, 200 mM NaCl, 1 mM EDTA, and 5 mM β-mercaptoethanol at pH 8.0 and 25°C. The alanine substitutions within the G1 peptide are underlined for clarity. NBD indicates no binding determined for the particular peptides either due to lack of any observable heat change or due to poor accuracy of ITC analysis involving such weak interactions ($K_d > 1$ mM). Errors were calculated from 3–4 independent measurements conducted at varying concentrations of cSH3 domain (50–200 μM) and peptides (2–8 mM) in order to further improve the accuracy of thermodynamic parameters. All errors are given to 1 standard deviation.

corresponding to homologous sites in Gab2 also implicate the role of E174 in the stability of these complexes (Harkiolaki *et al.*, 2009). In an attempt to explore the role of these acidic residues in the assembly of Grb2–Gab1 signaling complex, we measured and compared the binding of wild-type and various mutant cSH3 domains to peptides flanking G1 and G2 sites within Gab1 (Table 4). Our data reveal that alanine substitution of E171 within the cSH3 domain (cSH3_E171A) results in three- to fourfold reduction in affinity upon binding to both G1 and G2 sites, implying that E171 plays an important role in Grb2–Gab1 interaction at both G1 and G2 sites. In contrast, alanine substitution of E174 within the cSH3 domain (cSH3_E174A) completely abolishes binding, suggesting that E174 plays a critical role in Grb2–Gab1 interaction at both G1 and G2 sites. Furthermore, while alanine substitutions of D187 (cSH3_D187A) and D190 (cSH3_D190A) within the cSH3 domain have negligible effect on binding to G1 peptide, their binding to G2 peptide is concomitant with two- to fourfold reduction in affinity, indicating that both D187 and D190 are required for optimal Grb2–Gab1 interaction at G2 site but not at G1 site. Taken together, these data

Table 3. Thermodynamic parameters for the binding of cSH3 domain of Grb2 to single alanine mutants of Gab1-derived G2 peptide

Peptide	Sequence	*n*	K_d (μM)	ΔH (kcal/mol)	$T\Delta S$ (kcal/mol)	ΔG (kcal/mol)
G2	P**P**PVD**R**NL**K**PDR	0.94 ± 0.01	42 ± 1	−9.63 ± 0.05	−3.65 ± 0.03	−5.97 ± 0.02
G2_P − 5A	A**P**PVD**R**NL**K**PDR	1.08 ± 0.01	99 ± 6	−11.76 ± 0.64	−6.29 ± 0.68	−5.46 ± 0.03
G2_P − 4A	P**A**PVD**R**NL**K**PDR	NBD	NBD	NBD	NBD	NBD
G2_P − 3A	P**P**AVD**R**NL**K**PDR	1.11 ± 0.01	85 ± 1	−10.19 ± 0.07	−4.63 ± 0.07	−5.56 ± 0.01
G2_V − 2A	P**P**PAD**R**NL**K**PDR	1.05 ± 0.05	444 ± 15	−8.17 ± 0.28	−3.59 ± 0.26	−4.58 ± 0.02
G2_D − 1A	P**P**PVA**R**NL**K**PDR	1.06 ± 0.04	90 ± 1	−9.40 ± 0.13	−3.87 ± 0.13	−5.52 ± 0.01
G2_R0A	P**P**PVD**A**NL**K**PDR	NBD	NBD	NBD	NBD	NBD
G2_N + 1A	P**P**PVD**R**AL**K**PDR	1.15 ± 0.03	72 ± 3	−10.55 ± 0.45	−4.90 ± 0.48	−5.65 ± 0.03
G2_L + 2A	P**P**PVD**R**NA**K**PDR	1.09 ± 0.02	129 ± 3	−8.97 ± 0.19	−3.66 ± 0.20	−5.31 ± 0.01
G2_K + 3A	P**P**PVD**R**NL**A**PDR	NBD	NBD	NBD	NBD	NBD
G2_P + 4A	P**P**PVD**R**NL**K**ADR	NBD	NBD	NBD	NBD	NBD
G2_D + 5A	P**P**PVD**R**NL**K**PAR	1.08 ± 0.01	49 ± 2	−11.19 ± 0.33	−5.30 ± 0.36	−5.88 ± 0.02
G2_R + 6A	P**P**PVD**R**NL**K**PDA	0.94 ± 0.02	132 ± 1	−13.78 ± 0.75	−8.48 ± 0.75	−5.30 ± 0.01

The conserved residues within the PXXXRXXK motif in each peptide are bold-faced. All parameters were obtained from ITC measurements in a buffer of 50 mM Tris, 200 mM NaCl, 1 mM EDTA, and 5 mM β-mercaptoethanol at pH 8.0 and 25°C. The alanine substitutions within the G2 peptide are underlined for clarity. NBD indicates no binding determined for the particular peptides either due to lack of any observable heat change or due to poor accuracy of ITC analysis involving such weak interactions ($K_d > 1$ mM). Errors were calculated from 3–4 independent measurements conducted at varying concentrations of cSH3 domain (50–200 μM) and peptides (2–8 mM) in order to further improve the accuracy of thermodynamic parameters. All errors are given to 1 standard deviation.

Journal of Molecular Recognition

Table 4. Thermodynamic parameters for the binding of Gab1-derived peptides G1 and G2 to wild-type (WT) and various mutant cSH3 domains of Grb2

	G1 peptide				G2 peptide			
	K_d (μM)	ΔH (kcal/mol)	$T\Delta S$ (kcal/mol)	ΔG (kcal/mol)	K_d (μM)	ΔH (kcal/mol)	$T\Delta S$ (kcal/mol)	ΔG (kcal/mol)
cSH3_WT	152 ± 6	-3.22 ± 0.12	1.99 ± 0.09	-5.21 ± 0.02	42 ± 1	-9.63 ± 0.05	-3.65 ± 0.03	-5.97 ± 0.02
cSH3_E171A	444 ± 55	-3.83 ± 0.06	0.75 ± 0.02	-4.58 ± 0.07	158 ± 1	-7.48 ± 0.16	-2.28 ± 0.16	-5.19 ± 0.01
cSH3_E174A	NBD	NBD	NBD	NBD	NBD	NBD	NBD	NBD
cSH3_D187A	171 ± 8	-6.20 ± 0.02	-1.05 ± 0.05	-5.14 ± 0.03	182 ± 3	-3.54 ± 0.18	1.57 ± 0.19	-5.11 ± 0.01
cSH3_D190A	177 ± 17	-5.55 ± 0.33	-0.42 ± 0.27	-5.12 ± 0.06	77 ± 6	-7.11 ± 0.06	-1.49 ± 0.11	-5.62 ± 0.05

All parameters were obtained from ITC measurements in a buffer of 50 mM Tris, 200 mM NaCl, 1 mM EDTA, and 5 mM β-mercaptoethanol at pH 8.0 and 25°C. The various mutant constructs are E171A mutant of cSH3 domain (cSH3_E171A), E174A mutant of cSH3 domain (cSH3_E174A), D187A mutant of cSH3 domain (cSH3_D187A), and D190A mutant of cSH3 domain (cSH3_D190A). NBD indicates no binding determined for the particular SH3 domains either due to lack of any observable heat change or due to poor accuracy of ITC analysis involving such weak interactions ($K_d > 1$ mM). Errors were calculated from 3–4 independent measurements conducted at varying concentrations of cSH3 domain (50–200 μM) and peptides (2–8 mM) in order to further improve the accuracy of thermodynamic parameters. All errors are given to 1 standard deviation. Due to column constraints, the binding stoichiometries are not stated but they generally agreed to within ±10%.

suggest that E171 and E174 are likely involved in hydrogen bonding and/or salt bridging with arginine and/or lysine residues within the RXXK motifs at both G1 and G2 sites. Additionally, the binding of cSH3 domain at G2 site also requires D187 and D190 for optimal hydrogen bonding and/or salt bridging interactions, most likely with the C-terminal arginine residue within the PXVXRXLKPXR motif at G2 site.

Intermolecular ion pairing and counterion release drives the binding of cSH3 domain to G1 peptide but not to G2 peptide

Our data presented above strongly support a role of acidic and basic residues in driving Grb2–Gab1 interaction at both the G1 and G2 sites. In an attempt to decipher whether such charged residues are merely involved in intermolecular hydrogen bonding or exert their effect through the formation of intermolecular ion pairs or salt bridges, we analyzed the effect of salt on the binding energetics of cSH3 domain to G1 and G2 peptides (Figure 3). It is clearly evident from our data that the binding of cSH3 domain to G2 site displays no dependence on ionic strength with binding affinity of around 42 μM unaffected by changes in NaCl concentration in the 0–500 mM range (Figure 3a). In striking contrast, the binding of cSH3 domain to G1 site is dependent on ionic strength with binding affinity decreasing by about fourfold from a value of around 50 μM in the absence of NaCl to around 200 μM in the presence of 500 mM NaCl (Figure 3a). These observations suggest strongly that while the charged residues appear to be exclusively involved in the formation of intermolecular hydrogen bonding between the cSH3 domain and G2 peptide, they are also likely to be involved in the formation of intermolecular salt bridges between the cSH3 domain and G1 peptide. It should also be noted that the formation of salt bridges is coupled with the release of counterions and that such linked equilibrium is likely to play an important role in the binding of cSH3 domain at G1 site. To quantitatively measure the extent to which counterion release governs the binding of cSH3 domain at G1 site, we generated the salt linkage plot of $\ln K_d$ versus ln[NaCl] and calculated the fractional degree of net counterion release (ψ) from the corresponding slope of 0.34 ± 0.01 for G1 site (Figure 3a). It is believed that the release of counterions upon protein–ligand interactions can contribute to the overall free energy of binding in an entropically favorable or unfavorable manner. Indeed, such contribution to the overall free energy upon the release of counterions (ΔG_{ion}) decreases with increasing NaCl concentration in the 0–500 mM range and there is a penalty in counterion release of about +1 kcal/mol to the overall free energy for the binding of cSH3 domain to G1 peptide at high NaCl concentrations (Figure 3a). Consistent with these observations, while the underlying enthalpic (ΔH) and entropic ($T\Delta S$) contributions to the overall free energy (ΔG) for the binding of cSH3 domain to G1 peptide appear to be sensitive to changes in ambient salt concentration, the corresponding thermodynamic parameters display no such dependence for the binding of cSH3 domain to G2 peptide (Figure 3b). It is also noteworthy that classical SH3–ligand interactions are heavily dependent upon the formation of intermolecular salt bridges between oppositely charged residues flanking the PXXP motif and capping the binding groove within the β-barrel SH3 architecture (Lim *et al*., 1994; Yu *et al*., 1994; Sparks *et al*., 1996; Cesareni *et al*., 2002; McDonald *et al*., 2008a, 2009). Our findings above suggest that such electrostatic interactions may also play an important role in driving SH3–ligand interactions involving non-classical motifs such as RXXK (Mongiovi *et al*., 1999; Barnett *et al*., 2000; Kang *et al*., 2000; Kato *et al*., 2000; Lock *et al*., 2000; Urquhart *et al*., 2000; Lewitzky *et al*., 2001; Kami *et al*., 2002).

3D structural models provide contrasting insights into the distinct mechanisms employed by G1 and G2 motifs to recognize the cSH3 domain

To provide the physical basis of our findings reported here, we modeled the atomic structures of the cSH3 domain of Grb2 in complex with peptides containing the G1 and G2 motifs (Figure 4). Given the rather high sequence identity between the templates and targets, the modeled structures presented here can be relied upon with a very high degree of confidence. Nonetheless, caution must be exercised in that the conclusions drawn below are largely based on atomic models rather than atomic structures derived from direct experimental data.

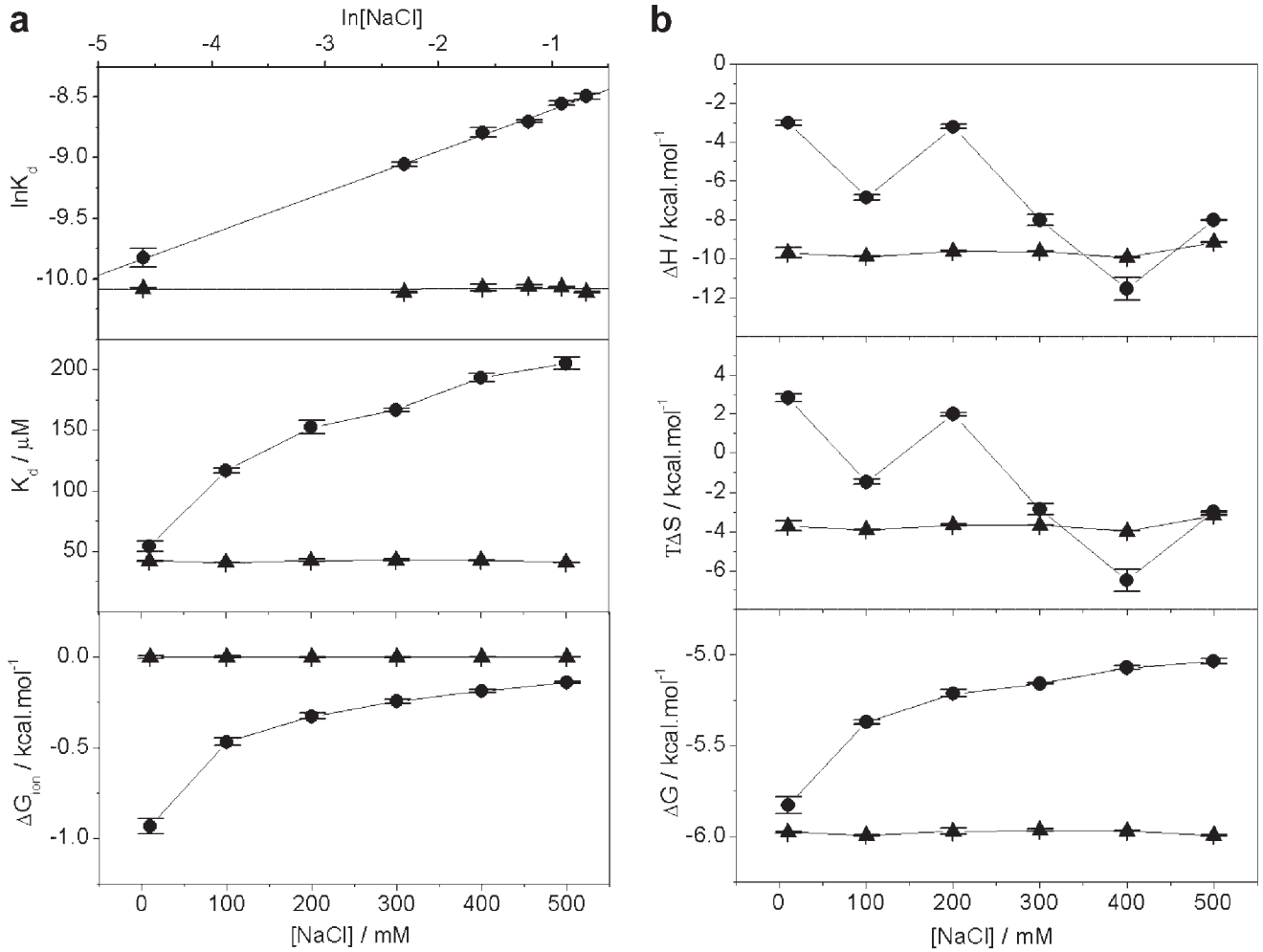

Figure 3. Effect of salt on the energetics of binding of cSH3 domain of Grb2 to Gab1-derived peptides G1 and G2 as analyzed by ITC. (a) Ln K_d versus ln[NaCl] plots (upper panel), K_d versus [NaCl] plots (middle panel), and ΔG_{ion} versus [NaCl] plots (lower panel) for the binding of cSH3 domain to G1 peptide (●) and G2 peptide (▲). In the upper panel, the solid lines show linear fits to the data points, while solid lines in the middle and lower panels are merely used to connect data points for clarity. (b) Dependence of thermodynamic parameters ΔH, $T\Delta S$, and ΔG on [NaCl] for the binding of cSH3 domain to G1 peptide (●) and G2 peptide (▲). The solid lines in all panels are merely used to connect data points for clarity. Each data point is the arithmetic mean of 3–4 independent experiments. All error bars are given to one standard deviation.

Notwithstanding these limitations, the modeled structures display the canonical β-barrel SH3 fold and accommodate the G1 and G2 peptides within the binding groove capped by RT loop on one side and n-Src loop on the other side. Although both G1 and G2 peptides share the same binding groove, the precise mechanisms by which they recognize it are distinct. Thus, while the G1 peptide adopts the relatively open PPII-helical conformation upon binding to the cSH3 domain (Figure 4a), the G2 peptide assumes a much tighter 3_{10}-helical conformation (Figure 4b). Remarkably, despite such distinguishing conformations, the nature of residues within the cSH3 domain involved in interacting with G1 and G2 peptides bear substantial similarities. Thus, the side chains of P − 2 in G1 peptide and P − 4 in G2 peptide occupy structurally equivalent positions and are stacked between benzyl side chain of F165 and phenyl side chain of Y209. Furthermore, the side chain guanidino and amino moieties of R0 and K + 3 residues constituting the RXXK motif within both G1 and G2 peptides hydrogen bond to side chain carboxylic oxygen atoms of E171 and E174 located within the RT loop in a tetrapartite manner. However, as noted above, R0 and K + 3 may also be involved in ion pairing with E171 and E174 in the case of binding of G1 peptide to the cSH3 domain due to the dependence of this SH3–peptide interaction on ionic strength (Figure 3). Importantly, aliphatic portions of R0 and K + 3 within both G1 and G2 peptides also, respectively, associate with benzyl side chain of F167 and side chain of W193 and thereby further stabilize the SH3–peptide interactions. Additional interactions are afforded by the side chains of P + 1 in G1 peptide and L + 2 in G2 peptide that stack between side chain amide moities of N192 and N208. Finally, the side chain of P + 4 in both the G1 and G2 peptides comes in close proximity to the side chain of M204 and likely adds to the overall stability of the complex. It should be noted that the binding of G2 peptide to the cSH3 domain is also characterized by a number of additional amino acid interactions that are absent in the binding of G1 peptide. Firstly, the side chain of V + 2 in G2 peptide associates with the side chains of F167, W193, and Y209. Secondly, the side chain guanidino moiety of R + 6 in G2 peptide likely hydrogen bonds with side chain carboxylic oxygen atoms of D187 and D190 in agreement with our data that alanine substitution of R + 6 reduces the binding affinity of G2 peptide by over threefold (Table 3). It is also noteworthy that although P − 1 and P + 2 residues are required

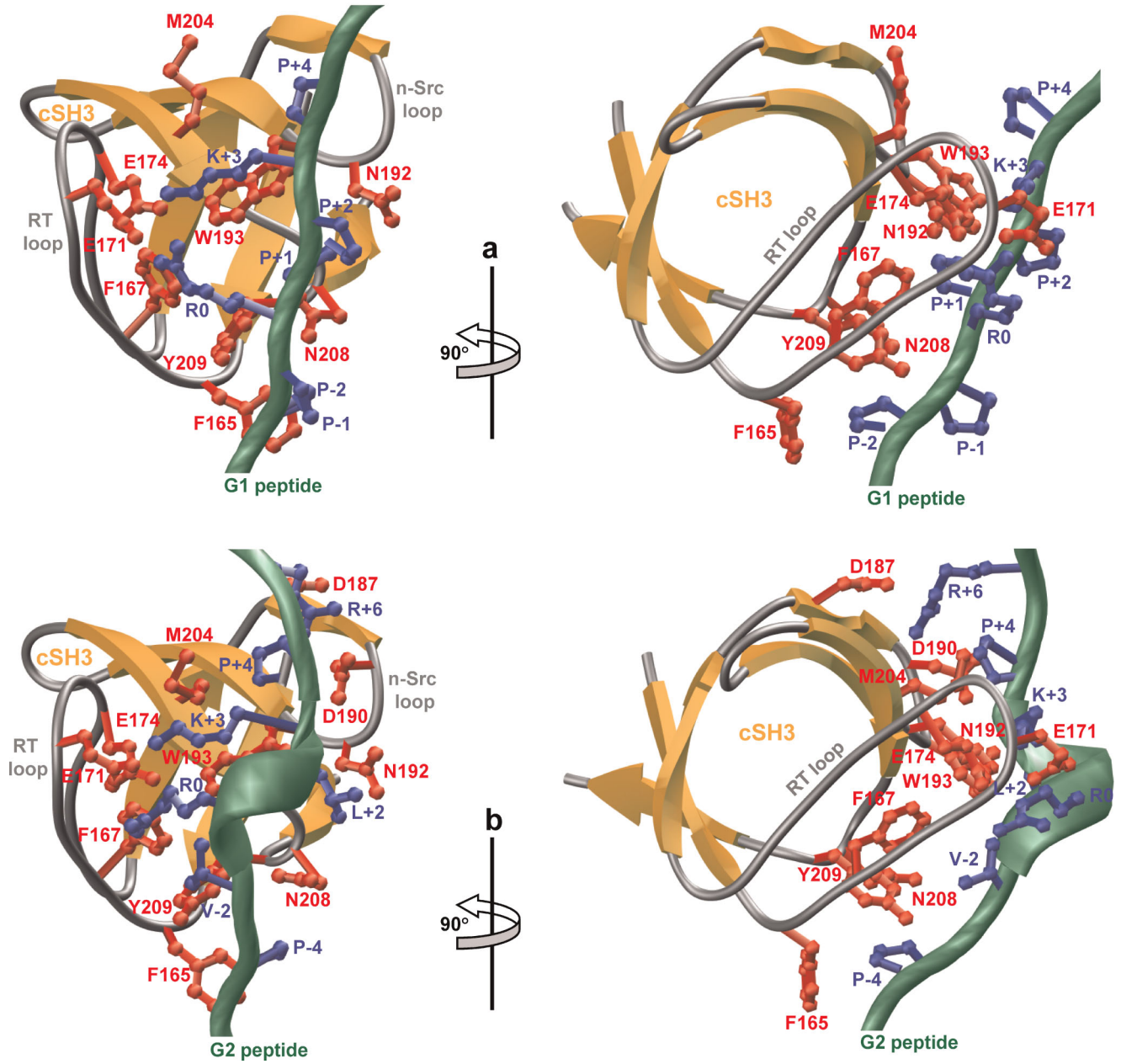

Figure 4. 3D structural models of the cSH3 domain of Grb2 in complex with Gab1-derived peptides G1 and G2. (a) Ribbon representation of the cSH3 domain bound to G1 peptide. The β-strands in the cSH3 domain are shown in yellow with loops depicted in gray and the side chains of key residues involved in making close contacts with the G1 peptide in red. The backbone of G1 peptide is colored green with the side chains of all residues within the PPRPPKP motif depicted in blue. (b) Ribbon representation of the cSH3 domain bound to G2 peptide. The β-strands in the cSH3 domain are shown in yellow with loops depicted in gray and the side chains of key residues involved in making close contacts with the G2 peptide in red. The backbone of G2 peptide is colored green with the side chains of conserved residues within the PXVXRXLKPXR motif depicted in blue.

for optimal binding of G1 peptide to cSH3 domain (Table 2), they point away from the binding groove within the cSH3 domain and are thus fully exposed to solvent. This likely implies that these residues are not directly involved in stabilizing the SH3–peptide complex through amino acid interactions but rather through their key role in imparting PPII-helical conformation on G1 peptide. Collectively, our 3D atomic models of cSH3 domain in complex with the G1 and G2 peptides suggest that a tight network of intermolecular hydrogen bonding, electrostatic and hydrophobic interactions underlie the strict requirement of amino acid residues within the corresponding PPRPPKP and PXVXRXLKPXR consensus motifs consistent with our thermodynamic analysis. Although water-mediated hydrogen bonding between the SH3 domain of Abl kinase and its proline-rich cognate ligands have been recently described (Palencia *et al*., 2004, 2010), water does not appear to play such a role in the binding of G1 and G2 motifs to the cSH3 domain of Grb2 (Harkiolaki *et al*., 2009).

PPRPPKP and PXVXRXLKPXR motifs show rarity in the human proteome

Due to the highly strict requirement of residues within G1 and G2 motifs for high-affinity binding of the cSH3 domain, it is likely that

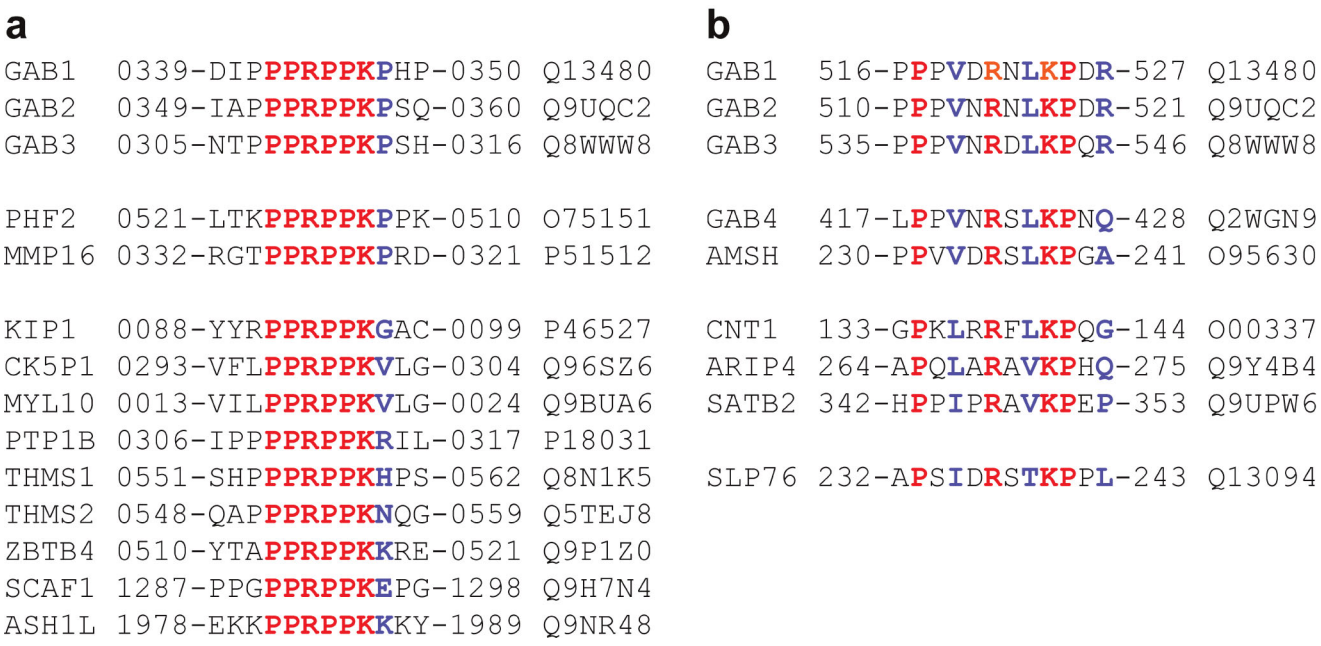

Figure 5. Amino acid sequence alignment showing the occurrence of PPRPPKP (a) and PXVXRXLKPXR (b) motifs in human proteome as identified through ScanProsite search at Expasy online server. Absolutely conserved residues within the motifs are shown in red, non-conserved residues within the motifs are depicted in blue, and all other residues are colored black. The proteins containing these motifs are listed in the left column and their corresponding Expasy codes are provided in the right column. The numerals hyphenated to amino acid sequence at each end denote the residue number within the protein sequence. Note that the amino acid sequences of PHF2 and MMP16 containing the PPRPPKP motif in (a) are provided in retro.

the Grb2–Gab1 interaction displays high fidelity in cellular signaling. In an attempt to test this hypothesis, we scanned the entire human proteome containing over 500 000 entries for the presence of PPRPPKP and PXVXRXLKPXR motifs (Figure 5). Our analysis reveals that both the G1 and G2 motifs are encountered in only a handful of proteins and that they are largely located in unstructured regions so as to facilitate their interactions with potential SH3 ligands. Importantly, these motifs are fully conserved in other members of Gab family of proteins, namely Gab2 and Gab3 but not Gab4, indicating that Gab4 may be functionally distinct from other Gab members. Interestingly, the PPRPPKP motif is also fully conserved in the PHD finger protein PHF2 and the matrix metalloprotein MMP16 that are unrelated to Gab family proteins. Whether binding of PHF2 and MMP16 to Grb2 is physiologically relevant remains to be determined. Notably, a number of other proteins also contain sequences similar to PPRPPKP motif but without the C-terminal proline, implying that they could also be potential cellular partners of Grb2. In contrast, PXVXRXLKPXR motif is strictly unique to Gab family proteins Gab1, Gab2, and Gab3, while Gab4 contains a related motif as does the zinc metalloprotease AMSH. However, neither Gab4 nor AMSH have been hitherto shown to be cellular partners of Grb2. Sequences related to the PXVXRXLKPXR motif but even more diverse from those encountered in Gab4 and AMSH are also encountered in several other proteins with the lymphocyte protein SLP76 being a notable example due to the fact that it has been shown to interact with the cSH3 domain of Grb2 in T cells (Jackman *et al*., 1995; Lewitzky *et al*., 2001). The ability of SLP76 to bind to the cSH3 domain of Grb2 suggests that although the PXVXRXLKPXR motif may be required for high-affinity binding, related sequences may also be potential cellular targets of Grb2.

CONCLUSIONS

Although Grb2–Gab1 is a key signaling complex involved in the transmission of extracellular information in the form of growth factors and cytokines to downstream targets such as transcription factors within the nucleus in a diverse array of cellular processes central to health and disease (Itoh *et al*., 2000; Sachs *et al*., 2000; Daly *et al*., 2002; Liu and Rohrschneider, 2002; Gu and Neel, 2003; Nishida and Hirano, 2003; Brummer *et al*., 2006; Ke *et al*., 2007; Bennett *et al*., 2008), the precise mechanism of its assembly remains hitherto unknown. Importantly, despite the discovery of an atypical RXXK sequence within Gab1 for the recruitment of Grb2 via its cSH3 domain over a decade ago (Lock *et al*., 2000; Lewitzky *et al*., 2001), the molecular determinants of this interaction have largely remained elusive to date. Our study shows that although Gab1 contains four distinct RXXK motifs, herein designated as G1, G2, G3, and G4, the cSH3 domain of Grb2 only recognizes the G1 and G2 motifs. Furthermore, we have also shown that the G1 and G2 motifs, respectively, conform to PPRPPKP and PXVXRXLKPXR consensus sequences for optimal binding to the cSH3 domain and that they employ distinct mechanisms. Thus, while G1 adopts a PPII-helical conformation in complex with cSH3 domain, G2 relies on a 3_{10}-helical conformation in agreement with the binding of homologous motifs in Gab2 to Grb2 (Harkiolaki *et al*., 2009). Additionally, our data also suggest that while the binding of cSH3 domain to G2 site is exclusively driven by hydrogen bonding and hydrophobic forces, binding at G1 site is additionally aided by the formation of intermolecular ion pairs between specific charged residues.

Given that we have relied here on short peptides to mimic RXXK motifs in Gab1, due largely to inherent difficulties

associated with isolation and purification of full-length protein, caution is warranted in that these motifs may depart from their physiological behavior when treated as short peptides due to the loss of local conformational constraints that they may be subject to in the context of full-length Gab1. Nonetheless, the fact that Gab1 contains two distinct sites for the binding of Grb2 raises the possibility for the formation of a signaling complex with a 2:1 stoichiometry – that is two molecules of Grb2 may associate with one molecule of Gab1 under physiological context. Supporting such a plausible scenario further is the evidence that Grb2 exists in dimer–monomer equilibrium in solution (McDonald *et al*., 2008b). Importantly, formation of $(Grb2)_2$–Gab1 signaling complex in the context of a cellular environment would be highly desirable as this would result in enhanced affinity and favorable energetics due to bivalent interaction between these two partners. In other words, Grb2 and Gab1 are likely to associate with each other at cellular concentrations in the submicromolar range in lieu of over tens of micromolar suggested by measurements between isolated G1 and G2 peptides and the cSH3 domain reported here. Accordingly, $(Grb2)_2$–Gab1 interaction may not only respond in a highly sensitive manner but may also be subject to fine tuning in response to specific extracellular stimuli. However, we note that the relatively weak binding of G1 and G2 motifs in the context of isolated peptides may also be due to the fact that they need to adopt into distinct conformations prior to binding to the cSH3 domain. Thus, it is conceivable that while these motifs pre-exist in appropriate conformations for binding to the cSH3 domain in the context of full-length Gab1, they become disordered in the context of isolated peptides. Such disorder is likely to encounter an energetic penalty upon the binding of G1 and G2 peptides to the cSH3 domain, rendering the apparent affinities much weaker than the intrinsic affinities.

Given that Grb2–Gab1 interaction plays a key role in coupling extracellular signals from cell surface RTKs such as HGFR, EGFR, FGFR, and PDGFR to downstream targets such as Ras and Akt (Liu and Rohrschneider, 2002; Gu and Neel, 2003; Nishida and Hirano, 2003), our new findings reported here bear particular significance to furthering our understanding of signaling through the Grb2–Gab1 complex at a molecular level. Of particular note is the fact that the activation of Ras and Akt pathways leads to down-regulation of the cell-cycle inhibitor p27Kip1 (Janes *et al*., 1994; Lim *et al*., 2000; Yang *et al*., 2000). Deregulation of p27Kip1 is believed to be one of the major factors contributing to the development of human breast cancer (Alkarain *et al*., 2004; Alkarain and Slingerland, 2004). Disruption of Grb2–Gab1 signaling complex may thus offer novel targets for the treatment of breast cancer. Our demonstration of the molecular details of the binding of cSH3 domain of Grb2 to two potential sites in Gab1 could spur interest in the development of novel therapeutic inhibitors toward this goal. Taken together, our data offer important insights into a key protein–protein interaction pertinent to cellular signaling and cancer.

Acknowledgements

This work was supported by funds from the National Institutes of Health (Grant# R01-GM083897) and the USylvester Braman Family Breast Cancer Institute to A.F. C.B.M. is a recipient of a postdoctoral fellowship from the National Institutes of Health (Award# T32-CA119929). B.J.D. and A.F. are members of the Sheila and David Fuente Graduate Program in Cancer Biology at the Sylvester Comprehensive Cancer Center of the University of Miami.

REFERENCES

Alkarain A, Slingerland J. 2004. Deregulation of p27 by oncogenic signaling and its prognostic significance in breast cancer. *Breast Cancer Res.* **6**: 13–21.

Alkarain A, Jordan R, Slingerland J. 2004. p27 deregulation in breast cancer: prognostic significance and implications for therapy. *J. Mammary Gland Biol. Neoplasia* **9**: 67–80.

Araki T, Nawa H, Neel BG. 2003. Tyrosyl phosphorylation of Shp2 is required for normal ERK activation in response to some, but not all, growth factors. *J. Biol. Chem.* **278**: 41677–41684.

Barnett P, Bottger G, Klein AT, Tabak HF, Distel B. 2000. The peroxisomal membrane protein Pex13p shows a novel mode of SH3 interaction. *EMBO J.* **19**: 6382–6391.

Bennett HL, Brummer T, Jeanes A, Yap AS, Daly RJ. 2008. Gab2 and Src co-operate in human mammary epithelial cells to promote growth factor independence and disruption of acinar morphogenesis. *Oncogene* **27**: 2693–2704.

Brannetti B, Via A, Cestra G, Cesareni G, Helmer-Citterich M. 2000. SH3-SPOT: an algorithm to predict preferred ligands to different members of the SH3 gene family. *J. Mol. Biol.* **298**: 313–328.

Brummer T, Schramek D, Hayes VM, Bennett HL, Caldon CE, Musgrove EA, Daly RJ. 2006. Increased proliferation and altered growth factor dependence of human mammary epithelial cells overexpressing the Gab2 docking protein. *J. Biol. Chem.* **281**: 626–637.

Carson M. 1991. Ribbons 2.0. *J. Appl. Crystallogr.* **24**: 958–961.

Cesareni G, Panni S, Nardelli G, Castagnoli L. 2002. Can we infer peptide recognition specificity mediated by SH3 domains? *FEBS Lett.* **513**: 38–44.

Chaires JB. 1996. Dissecting the free energy of drug binding to DNA. *Anticancer Drug Des.* **11**: 569–580.

Chardin P, Camonis JH, Gale NW, van Aelst L, Schlessinger J, Wigler MH, Bar-Sagi D. 1993. Human Sos1: a guanine nucleotide exchange factor for Ras that binds to GRB2. *Science* **260**: 1338–1343.

Cunnick JM, Meng S, Ren Y, Desponts C, Wang HG, Djeu JY, Wu J. 2002. Regulation of the mitogen-activated protein kinase signaling pathway by SHP2. *J. Biol. Chem.* **277**: 9498–9504.

Daly RJ, Gu H, Parmar J, Malaney S, Lyons RJ, Kairouz R, Head DR, Henshall SM, Neel BG, Sutherland RL. 2002. The docking protein Gab2 is overexpressed and estrogen regulated in human breast cancer. *Oncogene* **21**: 5175–5181.

Feng S, Chen JK, Yu H, Simon JA, Schreiber SL. 1994. Two binding orientations for peptides to the Src SH3 domain: development of a general model for SH3–ligand interactions. *Science* **266**: 1241–1247.

Ghose R, Shekhtman A, Goger MJ, Ji H, Cowburn D. 2001. A novel, specific interaction involving the Csk SH3 domain and its natural ligand. *Nat. Struct. Biol.* **8**: 998–1004.

Gu H, Neel BG. 2003. The "Gab" in signal transduction. *Trends Cell Biol.* **13**: 122–130.

Harkiolaki M, Tsirka T, Lewitzky M, Simister PC, Joshi D, Bird LE, Jones EY, O'Reilly N, Feller SM. 2009. Distinct binding modes of two epitopes in Gab2 that interact with the SH3C domain of Grb2. *Structure* **17**: 809–822.

Itoh M, Yoshida Y, Nishida K, Narimatsu M, Hibi M, Hirano T. 2000. Role of Gab1 in heart, placenta, and skin development and growth factor- and cytokine-induced extracellular signal-regulated kinase mitogen-activated protein kinase activation. *Mol. Cell Biol.* **20**: 3695–3704.

Jackman JK, Motto DG, Sun Q, Tanemoto M, Turck CW, Peltz GA, Koretzky GA, Findell PR. 1995. Molecular cloning of SLP-76, a 76-kDa tyrosine phosphoprotein associated with Grb2 in T cells. *J. Biol. Chem.* **270**: 7029–7032.

Janes PW, Daly RJ. deFazio A, Sutherland RL. 1994. Activation of the Ras signalling pathway in human breast cancer cells overexpressing erbB-2. *Oncogene* **9**: 3601–3608.

John B, Sali A. 2003. Comparative protein structure modeling by iterative alignment, model building and model assessment. *Nucleic Acids Res.* **31**: 3982–3992.

Kami K, Takeya R, Sumimoto H, Kohda D. 2002. Diverse recognition of non-PxxP peptide ligands by the SH3 domains from p67(phox), Grb2 and Pex13p. *EMBO J.* **21**: 4268–4276.

Kang H, Freund C, Duke-Cohan JS, Musacchio A, Wagner G, Rudd CE. 2000. SH3 domain recognition of a proline-independent tyrosine-based RKxxYxxY motif in immune cell adaptor SKAP55. *EMBO J.* **19**: 2889–2899.

Kato M, Miyazawa K, Kitamura N. 2000. A deubiquitinating enzyme UBPY interacts with the Src homology 3 domain of Hrs-binding protein via a novel binding motif PX(V/I)(D/N)RXXKP. *J. Biol. Chem.* **275**: 37481–37487.

Ke Y, Wu D, Princen F, Nguyen T, Pang Y, Lesperance J, Muller WJ, Oshima RG, Feng GS. 2007. Role of Gab2 in mammary tumorigenesis and metastasis. *Oncogene* **26**: 4951–4960.

Kim D, Chung J. 2002. Akt: versatile mediator of cell survival and beyond. *J. Biochem. Mol. Biol.* **35**: 106–115.

Lewitzky M, Kardinal C, Gehring NH, Schmidt EK, Konkol B, Eulitz M, Birchmeier W, Schaeper U, Feller SM. 2001. The C-terminal SH3 domain of the adapter protein Grb2 binds with high affinity to sequences in Gab1 and SLP-76 which lack the SH3-typical P-x-x-P core motif. *Oncogene* **20**: 1052–1062.

Li N, Batzer A, Daly R, Yajnik V, Skolnik E, Chardin P, Bar-Sagi D, Margolis B, Schlessinger J. 1993. Guanine-nucleotide-releasing factor hSos1 binds to Grb2 and links receptor tyrosine kinases to Ras signalling. *Nature* **363**: 85–88.

Lim WA, Richards FM, Fox RO. 1994. Structural determinants of peptide-binding orientation and of sequence specificity in SH3 domains. *Nature* **372**: 375–379.

Lim SJ, Lopez-Berestein G, Hung MC, Lupu R, Tari AM. 2000. Grb2 down-regulation leads to Akt inactivation in heregulin-stimulated and ErbB2-overexpressing breast cancer cells. *Oncogene* **19**: 6271–6276.

Liu Y, Rohrschneider LR. 2002. The gift of Gab. *FEBS Lett.* **515**: 1–7.

Lock LS, Royal I, Naujokas MA, Park M. 2000. Identification of an atypical Grb2 carboxyl-terminal SH3 domain binding site in Gab docking proteins reveals Grb2-dependent and -independent recruitment of Gab1 to receptor tyrosine kinases. *J. Biol. Chem.* **275**: 31536–31545.

Lohman TM, Mascotti DP. 1992. Thermodynamics of ligand–nucleic acid interactions. *Methods Enzymol.* **212**: 400–424.

Lowenstein EJ, Daly RJ, Batzer AG, Li W, Margolis B, Lammers R, Ullrich A, Skolnik EY, Bar-Sagi D, Schlessinger J. 1992. The SH2 and SH3 domain-containing protein GRB2 links receptor tyrosine kinases to ras signaling. *Cell* **70**: 431–442.

Marti-Renom MA, Stuart AC, Fiser A, Sanchez R, Melo F, Sali A. 2000. Comparative protein structure modeling of genes and genomes. *Annu. Rev. Biophys. Biomol. Struct.* **29**: 291–325.

Mayer BJ. 2001. SH3 domains: complexity in moderation. *J. Cell Sci.* **114**: 1253–1263.

McDonald CB, Seldeen KL, Deegan BJ, Farooq A. 2008a. Structural basis of the differential binding of the SH3 domains of Grb2 adaptor to the guanine nucleotide exchange factor Sos1. *Arch. Biochem. Biophys.* **479**: 52–62.

McDonald CB, Seldeen KL, Deegan BJ, Lewis MS, Farooq A. 2008b. Grb2 adaptor undergoes conformational change upon dimerization. *Arch. Biochem. Biophys.* **475**: 25–35.

McDonald CB, Seldeen KL, Deegan BJ, Farooq A. 2009. SH3 domains of Grb2 adaptor bind to PXpsiPXR motifs within the sos1 nucleotide exchange factor in a discriminate manner. *Biochemistry* **48**: 4074–4085.

Moeller SJ, Head ED, Sheaff RJ. 2003. p27Kip1 inhibition of GRB2–SOS formation can regulate Ras activation. *Mol. Cell Biol.* **23**: 3735–3752.

Mongiovi AM, Romano PR, Panni S, Mendoza M, Wong WT, Musacchio A, Cesareni G, Di Fiore PP. 1999. A novel peptide–SH3 interaction. *EMBO J.* **18**: 5300–5309.

Nishida K, Hirano T. 2003. The role of Gab family scaffolding adapter proteins in the signal transduction of cytokine and growth factor receptors. *Cancer Sci.* **94**: 1029–1033.

Odai H, Sasaki K, Iwamatsu A, Hanazono Y, Tanaka T, Mitani K, Yazaki Y, Hirai H. 1995. The proto-oncogene product c-Cbl becomes tyrosine phosphorylated by stimulation with GM-CSF or Epo and constitutively binds to the SH3 domain of Grb2/Ash in human hematopoietic cells. *J. Biol. Chem.* **270**: 10800–10805.

Palencia A, Cobos ES, Mateo PL, Martinez JC, Luque I. 2004. Thermodynamic dissection of the binding energetics of proline-rich peptides to the Abl-SH3 domain: implications for rational ligand design. *J. Mol. Biol.* **336**: 527–537.

Palencia A, Camara-Artigas A, Pisabarro MT, Martinez JC, Luque I. 2010. Role of interfacial water molecules in proline-rich ligand recognition by the Src homology 3 domain of Abl. *J. Biol. Chem.* **285**: 2823–2833.

Panni S, Dente L, Cesareni G. 2002. In vitro evolution of recognition specificity mediated by SH3 domains reveals target recognition rules. *J. Biol. Chem.* **277**: 21666–21674.

Park RK, Kyono WT, Liu Y, Durden DL. 1998. CBL–GRB2 interaction in myeloid immunoreceptor tyrosine activation motif signaling. *J. Immunol.* **160**: 5018–5027.

Record MT Jr, Lohman ML, De Haseth P. 1976. Ion effects on ligand–nucleic acid interactions. *J. Mol. Biol.* **107**: 145–158.

Robinson MJ, Cobb MH. 1997. Mitogen-activated protein kinase pathways. *Curr. Opin. Cell. Biol.* **9**: 180–186.

Rozakis-Adcock M, McGlade J, Mbamalu G, Pelicci G, Daly R, Li W, Batzer A, Thomas S, Brugge J, Pelicci PG, Schlessinger J, Pawson T. 1992. Association of the Shc and Grb2/Sem5 SH2-containing proteins is implicated in activation of the Ras pathway by tyrosine kinases. *Nature* **360**: 689–692.

Sachs M, Brohmann H, Zechner D, Muller T, Hulsken J, Walther I, Schaeper U, Birchmeier C, Birchmeier W. 2000. Essential role of Gab1 for signaling by the c-Met receptor in vivo. *J. Cell Biol.* **150**: 1375–1384.

Schaeper U, Gehring NH, Fuchs KP, Sachs M, Kempkes B, Birchmeier W. 2000. Coupling of Gab1 to c-Met, Grb2, and Shp2 mediates biological responses. *J. Cell Biol.* **149**: 1419–1432.

Seedorf K, Kostka G, Lammers R, Bashkin P, Daly R, Burgess WH, van der Bliek AM, Schlessinger J, Ullrich A. 1994. Dynamin binds to SH3 domains of phospholipase C gamma and GRB-2. *J. Biol. Chem.* **269**: 16009–16014.

Sparks AB, Rider JE, Hoffman NG, Fowlkes DM, Quillam LA, Kay BK. 1996. Distinct ligand preferences of Src homology 3 domains from Src, Yes, Abl, Cortactin, p53bp2, PLCgamma, Crk, and Grb2. *Proc. Natl. Acad. Sci. USA* **93**: 1540–1544.

Tong AH, Drees B, Nardelli G, Bader GD, Brannetti B, Castagnoli L, Evangelista M, Ferracuti S, Nelson B, Paoluzi S, Quondam M, Zucconi A, Hogue CW, Fields S, Boone C, Cesareni G. 2002. A combined experimental and computational strategy to define protein interaction networks for peptide recognition modules. *Science* **295**: 321–324.

Turnbull WB, Daranas AH. 2003. On the value of c: can low affinity systems be studied by isothermal titration calorimetry? *J. Am. Chem. Soc.* **125**: 14859–14866.

Urquhart AJ, Kennedy D, Gould SJ, Crane DI. 2000. Interaction of Pex5p, the type 1 peroxisome targeting signal receptor, with the peroxisomal membrane proteins Pex14p and Pex13p. *J. Biol. Chem.* **275**: 4127–4136.

Vidal M, Montiel JL, Cussac D, Cornille F, Duchesne M, Parker F, Tocque B, Roques BP, Garbay C. 1998. Differential interactions of the growth factor receptor-bound protein 2 N-SH3 domain with son of sevenless and dynamin. Potential role in the Ras-dependent signaling pathway. *J. Biol. Chem.* **273**: 5343–5348.

Wiseman T, Williston S, Brandts JF, Lin LN. 1989. Rapid measurement of binding constants and heats of binding using a new titration calorimeter. *Anal. Biochem.* **179**: 131–137.

Wyman J Jr. 1964. Linked functions and reciprocal effects in hemoglobin: a second look. *Adv. Protein Chem.* **19**: 223–286.

Yang HY, Zhou BP, Hung MC, Lee MH. 2000. Oncogenic signals of HER-2/neu in regulating the stability of the cyclin-dependent kinase inhibitor p27. *J. Biol. Chem.* **275**: 24735–24739.

Yu H, Chen JK, Feng S, Dalgarno DC, Brauer AW, Schreiber SL. 1994. Structural basis for the binding of proline-rich peptides to SH3 domains. *Cell* **76**: 933–945.

Zarrinpar A, Bhattacharyya RP, Lim WA. 2003. The structure and function of proline recognition domains. *Sci. STKE* **2003**: RE8.